A MATLAB-BASED GUI FOR REMOTE ELECTROOCULOGRAPHY VISUAL EXAMINATION

Tomas Stula[1], Antonino Proto[2], Jan Kubicek[2], Lukas Peter[2], Martin Cerny[2], Marek Penhaker[2]

[1]Laboratory of testing and measurement, Physical-Technical Testing Institute, Ostrava, Czech Republic

[2]Department of Cybernetics and Biomedical Engineering, VSB-TUO, Ostrava, Czech Republic

Abstract

In this work, a MATLAB-based graphical user interface is proposed for the visual examination of several eye movements. The proposed solution is algorithm-based, which localizes the area of the eye movement, removes artifacts, and calculates the view trajectory in terms of direction and orb deviation. To compute the algorithm, a five-electrode configuration is needed. The goodness of the proposed MATLAB-based graphical user interface has been validated, at the Clinic of Child Neurology of University Hospital of Ostrava, through the EEG Wave Program, which was considered as "gold standard" test. The proposed solution can help physicians on studying cerebral diseases, or to be used for the development of human-machine interfaces useful for the improvement of the digital era that surrounds us today.

Keywords

electrooculography; eye movement; view direction; orb deviation; eye blinking; MATLAB-based GUI

Introduction

Eye is source of electrical bio-potentials, which were first discovered by Du Bois Reymond in the previous century (1848) [1]. In the first half of 20th century, the electrical bio-potential of the eye was studied mainly with experimental meaning. Since the '50s, the clinical application of eye medicine began to engage scientists from all over the world. Firstly, the proposed method was the electroretinography (ERG), and over the years, its expansion brought many changes and further investigation techniques. Nowadays, methods for studying and analyzing eye movements concern a lot of research fields; from medicine to psychology, but also the art and advertisement research fields [2, 3]. In addition, the evaluation of the eye movement is common for developing human-machine interfaces in driving smart applications [4, 5]. There are many interpretation methods for describing the eye movements, such as video oculography (VOG), infrared oculography (IROG), scleral search coil (SSC) and electrooculography (EOG) [6, 7]. In medical diagnostics these methods enable the evaluation of objective examinations, such as eye muscles functionality, eyepiece asymmetry, eye movement during sleep or anesthesia, diagnosis of some vascular and neurological disorders, and retinopathies in pre-school children, among others [8–10].

The mentioned oculography methods differ for the practical approach on the evaluation of the eye movement. For instance, VOG method requires a camera for recording the movement; IROG follows the eye motion by measuring the amount of reflected light on the eye via a transmitter and a photodetector; SSC uses special lenses for the placement of the measuring inductor; and EOG acquires signals by means of electrodes placed around the eye. Among all, the SSC is the most invasive, the IROG have overtaken by VOG, while the EOG, although is the less accurate in terms of spatial resolution, is the only method able to follow the movements even with the eyelid closed [11].

In this work, we propose an EOG-based graphical user interface (GUI) able to display and recognize several types of eye movements. In literature, software tools for the evaluation of EOG signals mainly regard applications for the recognition of the common four directions for the eye view, such as up, down, left, and right, as well as to monitor the whole rotation of the eye [12]. The use of these tools is particularly useful for people suffering from neurological disorders because patients in locked-in state may not be able to speak or move but they could interact through an auditory

Lekar a technika – Clinician and Technology 2020, vol. 50(3), pp. 101–113, DOI: 10.14311/CTJ.2020.3.04
ISSN 0301-5491 (Print), ISSN 2336-5552 (Online)

communication system [13]. Moreover, software tools for the recognition of eye movements are used as standard interfaces for quadcopter navigation [14], and different techniques for baseline drift mitigation of the EOG signal are compared in the review proposed by Barbara et al. [15].

In the following paragraphs, firstly will be described the features characterizing the EOG signal, as well as the technical approaches for its analysis. Then, the main parts of the proposed system will be introduced, by focusing particularly on the way to detect the eye movement, to remove undesirable artifacts, and the way to draw the trajectory and to calculate the orb deviation. Finally, tests carried out for the proper evaluation of the system functioning will be listed, and the conclusion paragraph ends the paper.

Electrooculography

EOG signals and artifacts

EOG records the so-called inactive eye potentials, those arising from spontaneous or controlled movement of the eye. It measures the differences of the electrical potential generated between the cornea, i.e. positively charged, and the retina, i.e. negative charged (Fig. 1). These differences of electrical potential cause changes in the electrostatic field when the eye is moving [16]. By placing electrodes surrounding the eye, we acquire the electrical signals related to eye movements [17]. Electric dipole is oriented following the antero-posterior axis of eye bulb, and its orientation slightly deviates from the optical axis when the eye moves. Therefore, the magnitude of the potential difference changes with direct dependence on the amplitude of the rotation.

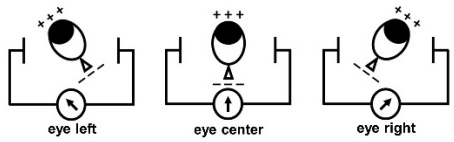

Fig. 1: Change of cornea and retina electric dipole.

The EOG signal is random; any mathematical equation cannot describe it. It depends on the eye motion activity and on the current state of a person. The frequency range of the signal is approximately from 0.5 to 15 Hz, and voltage values do not exceed the millivolt units: the range of values is approximately from 50 to 3500 μV. The EOG method can evaluate the eye rotation within a range of ±70° with an accuracy of approximately 1.5–2°. The eye rotation of about 1° corresponds to a voltage variation of approximately 20 μV, and there is an almost linear dependency between the horizontal angle of the optical axis and the EOG measured signal, up to approximately ±30° [7, 18].

Artifacts can significantly distort the EOG signal: there are two categories grouping them based on the nature of the source: (1) physical artifacts, and (2) biological artifacts. Several factors can generate artifacts of the former category, such as the aging of the electronic instrumentation, and the presence of electrostatic or electromagnetic fields in the space surrounding the measurement area [19]. In addition, in this category, there are artifacts caused by the movement of electrodes. The latter category refers to many biological aspects related to the human physiology [20]. In addition, the activity of muscles generates artifacts, which can occur if the patient is nervous or worried, or while biting and swallowing, among other activities that involve facial muscles. Again, the heart activity influences the EOG signal if the electrode placement is close to any artery. In this case, the EOG signal changes synchronously with the pulse because the electrode displacement causes a change on its impedance value. Moreover, the breathing, or the sweating can generate artifacts. It is possible to remove artifacts both in time and frequency domains, but the best solution should be to avoid their occurrence [21, 22].

In the solution proposed here, the algorithm automatically removes artifacts arising from eye blinking, heart, and muscle activities, as well as the network interference and high amplitude output signals.

Approaches for the analysis of EOG signals

The analysis in the time domain concerns the study of changes in the amplitude of the EOG signals. It is possible to determine the values of amplitude, slope, and period of the signal, as well as the trajectory of motion, which is useful to calculate the rate of eye movement changes. The time domain approach uses geometric and numerical methods, such as correlation, statistics, and artificial neural network techniques. The correlation functions, i.e. autocorrelation and correlation, are used for the temporal localization of a specific movement event [18]. Statistical method is useful for analyzing EOG measurements performed for an extended period, usually twenty-four hours. Again, machine learning techniques may enable the simulation of the human thinking, since its basic and essential feature is about the ability to learn [23]; indeed, it is possible to combine information on EEG and EOG data for using convolutional neural networks to enable the early diagnosis of neurological disorders [24].

The classical Fourier transform converts signals from the time domain to the frequency one. Its practical use is for stationary signals but the EOG signal is a non-stationary one. To extend the use of the frequency domain for the analysis of eye movement, it is suggested to use window functions that operate on the time-frequency domain. The window functions provide information on the frequency distribution at different time intervals, and the wavelet transform allows to use windows with progressive widths enabling a multireso-

Lekar a technika – Clinician and Technology 2020, vol. 50(3), pp. 101–113, DOI: 10.14311/CTJ.2020.3.04
ISSN 0301-5491 (Print), ISSN 2336-5552 (Online)

lution analysis [25, 26]. In this way, it is possible to separate the different signal components, whose frequency spectra overlap.

System Concept

Fig. 2 shows the diagram of the proposed system [27]. The algorithm is composed by five blocks. The input signals are four: from EOG1 to EOG4.

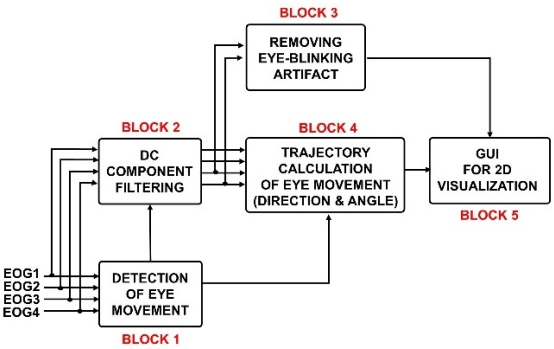

Fig. 2: Diagram of the proposed system.

BLOCK 1 – Detection of eye movement

The goal of BLOCK 1 is to detect the eye movement. As it is visible in Fig. 3, the algorithm firstly differentiates the horizontal and vertical EOG components:

$$\begin{cases} X1 = EOG1 - EOG2 \\ Y1 = EOG4 - EOG3 \end{cases} \quad (1)$$

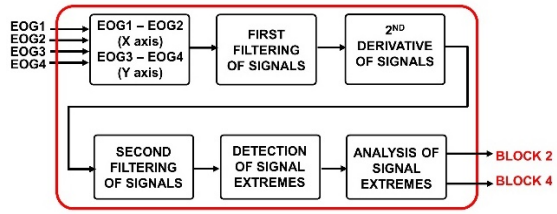

Fig. 3: Diagram of BLOCK 1.

Then, X1 and Y1 undergo a low pass filtering by means of a square convolution function to eliminate the high frequency noise, the facial muscle artifacts, and the network interference (Fig. 4).

Hence, the algorithm makes a 2nd derivative of X2 and Y2 to find out the acceleration values, which indicate the eye movement activity. Again, a filtering of X3 and Y3 occurs by means of a sine convolution function to highlight the maximum and minimum values, which are shown in X4 and Y4 of Fig. 4.

Then, the algorithm must detect the parts of EOG signals having two established sequences of area polarities: '+ - +', and '- + -' (enlargement in Fig. 4, i.e. Y4). The detection of their local extremes (beginning and end of eye movement) occurs through the definition of two thresholds, which were suggested by physicians at the Clinic of Child Neurology of University Hospital of Ostrava.

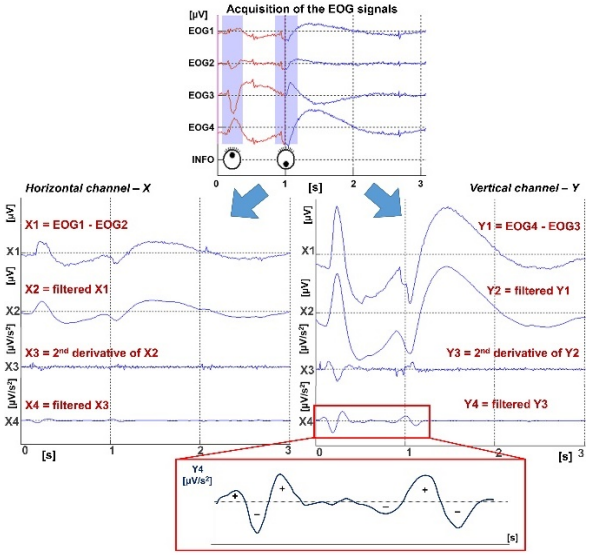

Fig. 4: The first steps to detect the eye movement.

In Supplementary Materials, Fig. 1S shows the diagram related to the algorithm part in which the system recognizes the period where the eye movement occurs, i.e. Y5: interval <a,b>, and the maximum and minimum values, i.e. C1, C2, and C3, shown in Fig. 5.

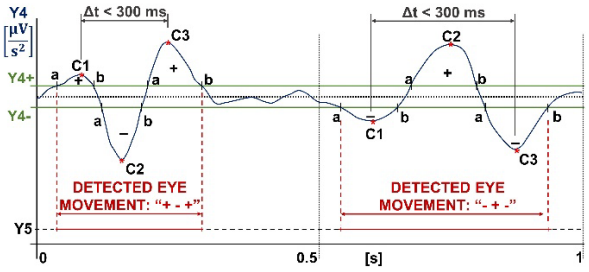

Fig. 5: Detected time interval of eye movement.

The eye movement occurs only if the interval time between extremes C1 and C3 is less than 300 ms. This value was established experimentally, by testing the system when the user was performing ten elementary eye movements, as it follows: (1) centre-right-centre; (2) centre-left-centre; (3) centre-top-centre; (4) centre-down-centre; (5) centre-top right corner-centre; (6) centre-top left corner-centre; (7) centre-bottom right corner-centre; (8) centre-bottom left corner-centre; (9) centre-right-left-centre; (10) centre-top-down-centre. Table 1S (Supplementary Materials) shows the values of the interval time between extremes C1 and C3 for the mentioned tests. The maximum value is 289 ms, while the minimum is 179 ms.

About the horizontal component of the EOG signal, it is X5 (Fig. 6). It can happen that X5 and Y5 do not overlap each other on the same time window. Also, it can happen to find a time interval corresponding to

Lekar a technika – Clinician and Technology 2020, vol. 50(3), pp. 101–113, DOI: 10.14311/CTJ.2020.3.04
ISSN 0301-5491 (Print), ISSN 2336-5552 (Online)

a component, X or Y, but not to the other one. So, it was necessary to create a method to merge X5 and Y5 together.

Fig. 6 shows the way for merging these time intervals. The result is the interval <x, y>. If this value is less than 600 ms, the time interval corresponds to the detected eye movement. Conversely, if the value is greater than 600 ms, a fixed time interval of 600 ms is always set from the beginning of such detected eye movement.

The output of the BLOCK 1 consists in the detection of the time interval corresponding to the performed eye movement.

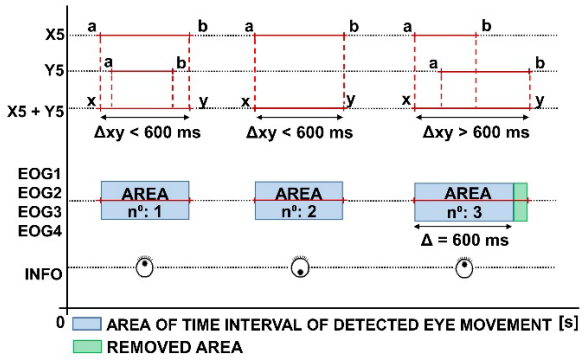

Fig. 6: Method to merge the detected time interval on the X and Y components.

BLOCK 2 – DC component filtering

For the proper visualization of EOG signals, we need to delete the offset error due to the constant DC component. In BLOCK 2, signal filtering occurs through to the use of a third order high-pass Butterworth filter with cut-off frequency of 0.1 Hz. In MATLAB, such a filter is described by a differential equation computed by the filtfilt function.

BLOCK 3 – Removing eye blinking artifact

The eye blinking is an artifact due to the contraction of the muscle fibres of the upper eyelid, and it mainly affects EOG3 and EOG4 signals since the electrodes for their acquisition are placed above and below the eye. For this reason, as inputs of BLOCK 3 we have only EOG3 and EOG4, and the method used to detect this artifact relies on the calculation and comparison of signal areas along an established time-interval (Fig. 7). The blue lines represent signals before removing DC component.

In Fig. 7, AREA 3, i.e. S3, is much larger than AREA 4, i.e. S4. Indeed, eye blinking artifacts occur only if the ratio between S3 and S4 is greater than an empirical value, which is approximated to 2.8.

$$\frac{S3}{S4} = \frac{\int_{t1}^{t2} |EOG3(t)|dt}{\int_{t1}^{t2} |EOG4(t)|dt} > 2.8 \qquad (2)$$

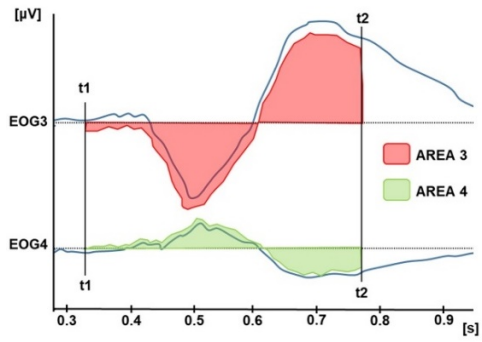

Fig. 7: Detected areas corresponding to eye blinking.

This empirical value is the result obtained while performing diverse types of eye blinking in the form of single wink, wink repeated two and three times, and spontaneous and forced wink [27]. Table 2S (Supplementary Materials) shows the results obtained for all the diverse eye blinking.

BLOCK 4 – Trajectory calculation of eye movement

As input of BLOCK 4, there are the EOG signals without the DC component, and the output result of BLOCK 1 that returns the time intervals corresponding to the detected area of the eye movement.

Fig. 8 shows the block diagram representing the steps used to calculate the eye trajectory, in terms of direction and orb deviation.

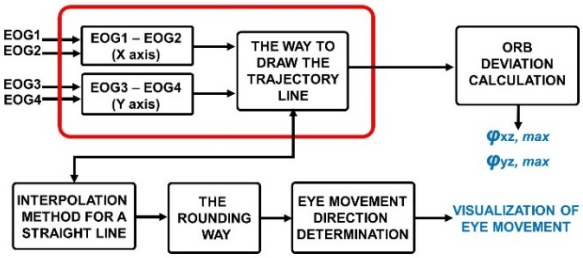

Fig. 8: Diagram of BLOCK 4.

Firstly, the algorithm makes a mutual subtraction of EOG signals for both the X (EOG1–EOG2) and Y (EOG4–EOG3) components, so to obtain a sequence of point coordinates, i.e. $[X_n, Y_n]$, shown in Fig. 9. Then, it calculates the equation of the line passing through the centre of a Cartesian system, for which the sum of distances D_0 to D_n, from all $[X_n, Y_n]$ points, is minimal. In this way, it is possible to draw the line of the eye movement and determine the view angle value. It occurs by means of three subsequent approximations (Fig. 9). As result of the third approximation, we obtained a resolution of 0.72° for the calculation of the view angle.

To determine the direction and verse of eye movement, the algorithm proceeds as follows. As it is shown in Fig. 10, the possible directions are four (up, down,

Lekar a technika – Clinician and Technology 2020, vol. 50(3), pp. 101–113, DOI: 10.14311/CTJ.2020.3.04
ISSN 0301-5491 (Print), ISSN 2336-5552 (Online)

left and right), and to find out the proper direction, it calculates the minimum value of the difference given by "$\Delta = |\alpha - \beta|$".

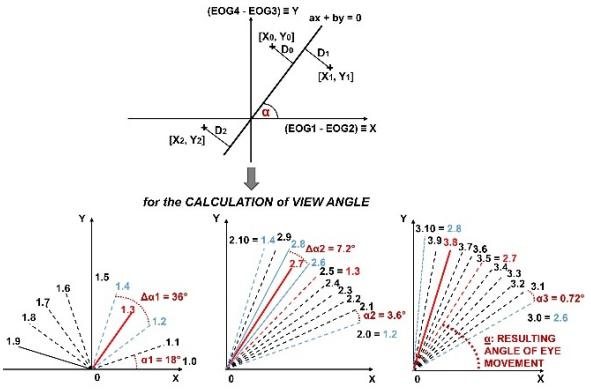

Fig. 9: Determination of the angle of view by means of successive approximations.

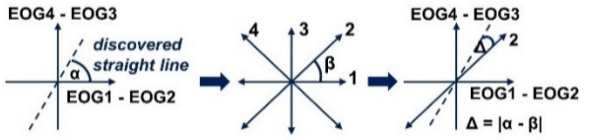

Fig. 10: Determination of the direction of the trajectory line.

To determine the verse of eye movement, which can be either positive or negative, the algorithm counts the positive and negative distances between eye trajectory points, i.e. $[X_0 \ldots X_n, Y_0 \ldots Y_n]$; a straight-line *q*, which passes through centre, and it is normal-line *p*.

Fig. 11 shows the decision rule for the evaluation of the verse of eye movement.

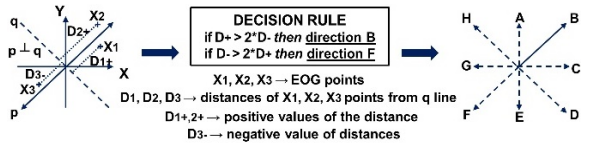

Fig. 11: Determination of the verse of the trajectory line.

To determine the value of orb deviation, the algorithm needs to calculate the maximum value of amplitude deviation for both X and Y components, which are $\Delta EOG_{X,max}$ and $\Delta EOG_{Y,max}$, respectively. It is due to linear dependence, up to ±30°, between orb deviation, from optical axis "z" (Fig. 12), and amplitude of EOG signal [7].

It implies that $\Delta EOG_{X,max}$ corresponds to orb deviation on X channel, i.e. $\varphi_{XZ,max}$, and $\Delta EOG_{Y,max}$ to the $\varphi_{YZ,max}$, respectively. Because the maximum value of orb deviation is approximately ±45°, we found out that the maximum amplitude deviation is up to ±300 μV. Thus, it is easy determine a resolution of 6.6 μV/° for the calculation of the orb deviation.

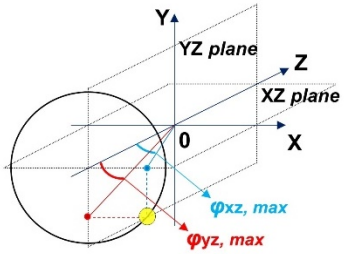

Fig. 12: Determination of orb deviation values (3D space).

BLOCK 5 – GUI for 2D visualization

MATLAB, version R2013a, was used for developing the GUI. Before running the software, it is necessary to set the access path to the directory in which the boot program is stored. Then, by opening the EOG data file, it is possible to observe the main window of the GUI (Fig. 13).

It contains two graphs: the former displays all the EOG channels: from EOG1 to EOG4, and an "INFO" line, which shows the graphical representations of the eye movements, corresponding to the purple-marked areas (i.e. detected eye movements). Below this graph, the buttons have the following meaning: "Zoom out", and "Zoom in" will reduce the time scale by half, and increase it by the double, respectively. The arrows "<—" and "—>" serve to move the signals by a second in the corresponding direction. By clicking "<<<——" and "——>>>" arrows, signals are shifted with a magnitude equals to the entire time slot. Conversely, "Reduce", and "Expand" buttons adjust the amplitude values. The sensitivity value is displayed between these buttons, and the default value is ±400 μV, i.e. 200 μV/div.

The latter graph represents the calculated trajectory of the eye movement, corresponding to the selected time interval in the upper graph. In such time interval of the upper graph, all channels are marked with red lines.

The time interval can be set by buttons, or by means of mouse clicking. The "<—" and "—>" arrows serve to scroll the entire interval by 0.1 s in the corresponding direction, while "<<<——" and "——>>>" serve to select the boundaries of the interval: its beginning and its end. In such a graph, the variations of the amplitude difference EOG 1-EOG 2 are plotted on the x-axis, while the variations of the amplitude difference EOG 4-EOG 3 are on the y-axis. Again, the change of the trajectory colour, i.e. from red to yellow, shows the time sequence of the performed eye movement. As already mentioned, the result of the calculation displayed in this graph relates to the selected interval in the upper graph, for which the boundaries indicate the beginning and the end of the purple-marked area. Moreover, the eye symbol on the right side of the

Lekar a technika – Clinician and Technology 2020, vol. 50(3), pp. 101–113, DOI: 10.14311/CTJ.2020.3.04
ISSN 0301-5491 (Print), ISSN 2336-5552 (Online)

bottom graph shows the direction of the eye view, and the corresponding angle value is then calculated and displayed next to the symbol.

Again, by clicking the "Detection of intervals" button, the GUI displays a graph showing the progressive analysis made on the EOG signals to detect the time interval for which the eye movement occurs (Fig. 2S in Supplementary Materials). Moreover, in the main window of the GUI, the "DC component" button displays the result of the DC component filtering (Fig. 3S in Supplementary Materials).

The executable file about the MATLAB-based GUI for remote electrooculography visual examination, can be asked to the corresponding author of this manuscript.

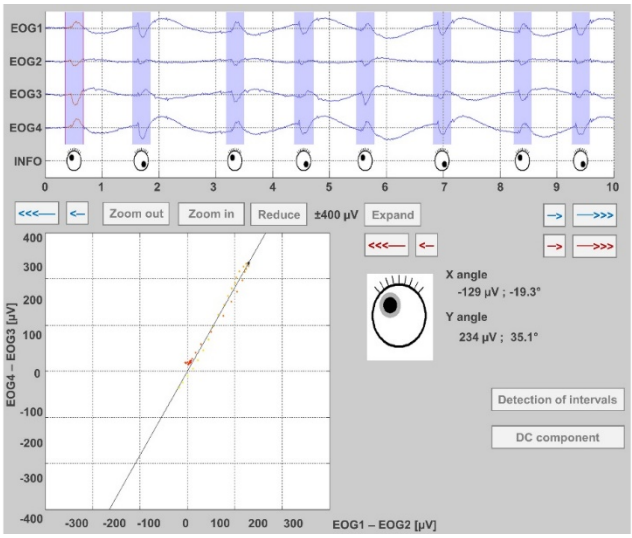

Fig. 13: Main window of the developed GUI.

Testing and Evaluation

To test and evaluate the MATLAB-based GUI for the visual examination of the EOG signals, a healthy male user (age: 27-year, body weight: 75 kg, height: 186 cm) was recruited to perform the experiment at the Clinic of Child Neurology of University Hospital of Ostrava. Twenty eye movements were carried out, in the form of: (1) centre-right-centre; (2) centre-left-centre; (3) centre-top-centre; (4) centre-down-centre; (5) centre-right-left; (6) centre-top-down; (7) centre-right-centre, second time; (8) left-right-eye blink; (9) centre-top-centre, second time; (10) centre-down-centre, second time; (11) centre-top right corner-centre; (12) centre-top left corner-centre; (13) centre-bottom right corner-centre; (14) centre-bottom left corner-centre; (15) centre-left-right-centre; (16) centre-top-down-eye blink; (17) double eye blink, repeated two times; (18) an eye blink, repeated three times; (19) an eye blink; (20) an eye blink, second time. Fig. 14 shows the placement of the five sensing electrodes for testing the proposed algorithm.

For measuring the horizontal signal components, the electrodes were placed on the left and right corner of the eyes (electrodes 1 and 2). For measuring the vertical components, the electrodes were placed above and below the eye (electrodes 3 and 4). The reference electrode was placed in the middle of forehead (electrode 5).

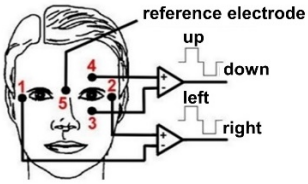

Fig. 14: Electrodes placement for the acquisition of EOG signal.

While carrying out the experiment, the user was seated, and a nurse was gradually read each single physical eye movement carried out in the experiment.

Fig. 15 shows one of the eye movement listed above. It is the movement number (18) an eye blink, repeated three times.

Table 1 lists the values of orb deviation calculated for all the twenty measured eye movements.

To validate the proposed system, the obtained results were verified by means of the EEG Wave Program, DEYMED Diagnostic s.r.o., formerly Alien technik s.r.o. [28]. This software serves primarily to monitoring EEG signals, but also allows the simultaneous examination of EOG, EMG, and ECG waveforms: it is used for polygraph examination. A great advantage of the EEG Wave Program is the ability to record video images while the person is performing the experiment. These video images are synchronized with the EOG channels, allowing easy visual examination of the movements.

Lekar a technika – Clinician and Technology 2020, vol. 50(3), pp. 101–113, DOI: 10.14311/CTJ.2020.3.04
ISSN 0301-5491 (Print), ISSN 2336-5552 (Online)

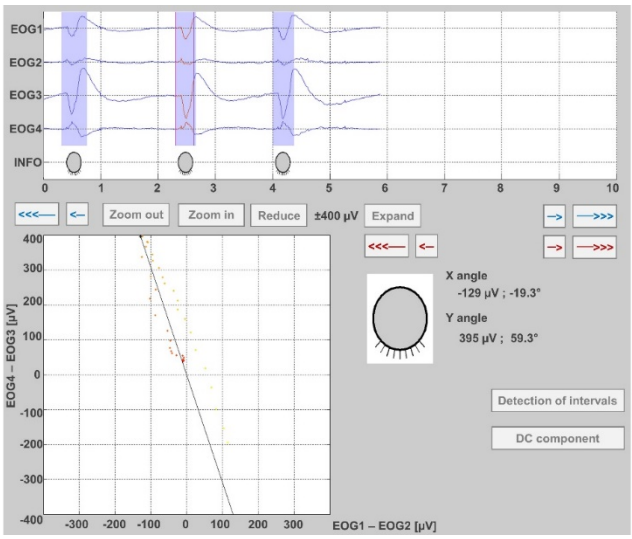

Fig. 15: Result for test regarding eye movement number (18) an eye blink, repeated three times.

Table 1: Values of calculated orb deviation for the twenty measured eye movements.

Eye mov. #	First eye movement				Second eye movement			
	Horizontal plane		Vertical plane		Horizontal plane		Vertical plane	
	$\Delta EOG_{X,max}$ (µV)	$\varphi_{XZ,max}$ (°)	$\Delta EOG_{Y,max}$ (µV)	$\varphi_{YZ,max}$ (°)	$\Delta EOG_{X,max}$ (µV)	$\varphi_{XZ,max}$ (°)	$\Delta EOG_{Y,max}$ (µV)	$\varphi_{YZ,max}$ (°)
1	243	36.5	54	8.1	-245	-36.7	-80	-12
2	-222	-33.3	20	3.1	238	35.6	0	0
3	49	7.3	220	32.9	-12	-1.8	-191	-28.6
4	-20	-2.9	-122	-18.2	75	11.3	210	31.5
5	214	32	69	10.4	-351	-52.6	-56	-8.4
6	101	15.2	395	59.3	-8	-1.2	-247	-37.1
7	283	42.4	91	13.7	-215	-32.1	-78	-11.6
8	-212	-31.8	19	2.9	223/-44	33.5/-6.6	-15/195	-2.2/29
9	47	7.1	213	32	-1	-0.1	-143	-21.4
10	-30	-4.4	-101	-15.1	70	10.5	178	26.7
11	149	22.3	271	40.7	-108	-16.1	-148	-22.1
12	-103	-15.5	173	26	89	13.3	-163	-24.4
13	170	25.6	-6	-0.9	-88	-13.2	77	11.5
14	-113	-16.9	-62	-9.3	235	35.3	139	20.9
15	144	21.5	36	5.5	-320	-47.9	-72	-10.7
16	63	9.5	285	42.7	-32/61	-4.8/9.2	-199/189	29.8/28
17	-73/-48	-10.9/-7.2	223/302	33.4/45	-133/-67	-20/-10	335/297	50.2/44
18	-99	-14.8	382	57.3	-129/-125	-19.3/-18	395/429	59.3/64
19	-20	-3	315	47.3	-	-	-	-
20	-9	-1.3	273	40.9	-	-	-	-

$\Delta EOG_{X,max}$ – EOG1 and EOG2 potential difference change; $\varphi_{XZ,max}$ – orb deviation from optical axis in XZ plane;
$\Delta EOG_{Y,max}$ – EOG4 and EOG3 potential difference change; $\varphi_{YZ,max}$ – orb deviation from optical axis in YZ plane.

The proposed algorithm was successfully validated thanks to the EOG data measured by the EEG Wave Program, which also recorded video images of the experiment (Fig. 4S, Supplementary Materials). Indeed, by using such EOG data and video recording, the accuracy and reliability of the results given by the designed algorithm, implemented into the MATLAB-based GUI, were verified in the time domain. Thus, it can be stated that the obtained results correspond to the actual physical movements of the eye.

Lekar a technika – Clinician and Technology 2020, vol. 50(3), pp. 101–113, DOI: 10.14311/CTJ.2020.3.04
ISSN 0301-5491 (Print), ISSN 2336-5552 (Online)

Fig. 5S (Supplementary Materials) shows the EOG signals acquired by means of the EEG Wave Program for the eye movements number (18) single eye blink, three times.

Conclusion

The developed MATLAB-based GUI allows the remote analysis of the eye movements through the acquisition of four EOG signals. The designed software is based on a step-by-step algorithm, which allow to display information on view direction and orb deviation of the eye movements. Physicians can use this tool for studying cerebral disease of patients. Indeed, while patients are sleeping, EOG signals of laxation state may predict neurological cerebral dysfunction. In addition, the proposed algorithm can be used for designing human-machine interfaces useful to improve the life quality of people with disabilities, because in the current digital era, there is a growing need to have technologies to improve the health-care system.

The goodness of the algorithm developed in this work has been validated at the Clinic of Child Neurology of University Hospital of Ostrava.

Acknowledgement

This work is supported in part by 'Biomedical Engineering systems XVI' project, grant number: SV4500X21/2101, SP2020/55; and in part by the ESF for international mobility, grant number: CZ.02.2.69/0.0/0.0/18_070/0010219.

The authors thank all physicians at the Clinic of Child Neurology of University Hospital of Ostrava, who supported and contributed with valuable advices to the development of the algorithm useful for the design of the MATLAB-based GUI for remote electro-oculography visual examination.

Supplementary Materials

Fig. 1S shows the block diagram on the algorithm part in which the system recognizes the period where the eye movement occur, i.e. interval <a,b>, and also the maximum and minimum points, i.e. C1, C2, and C3.

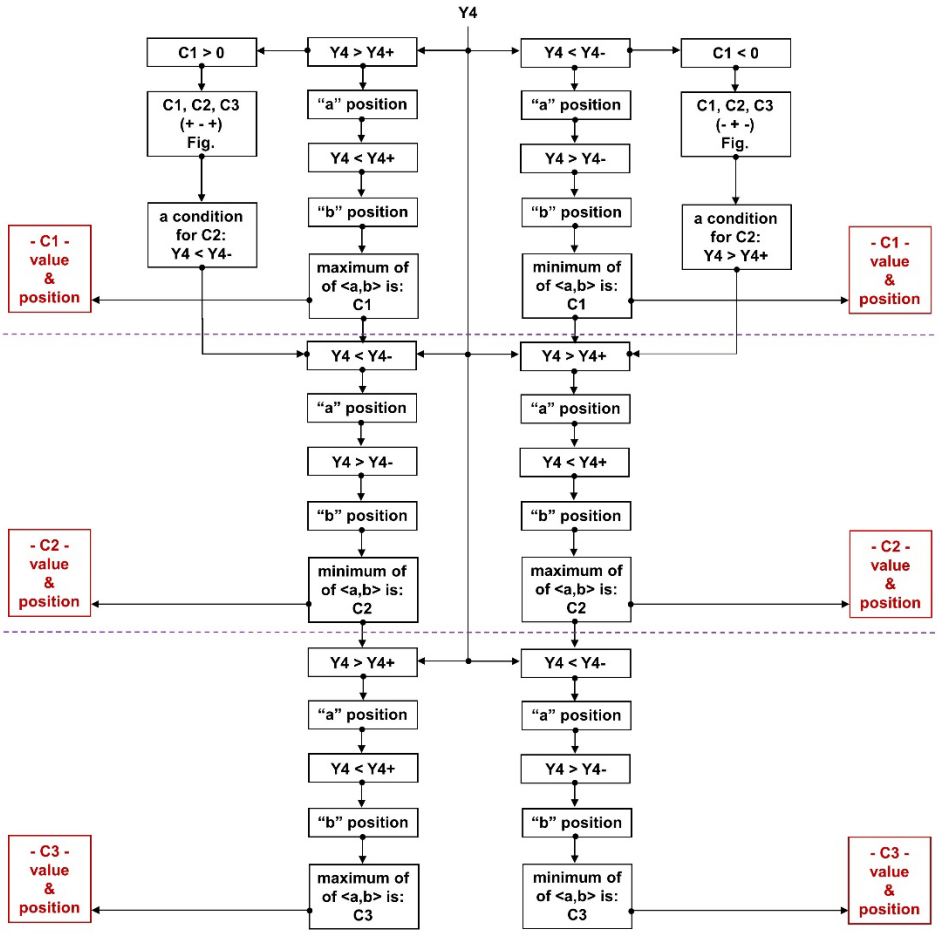

Fig. 1S: Block diagram showing the algorithm part for the recognition of the period of eye movement.

Table 1S shows the values of the interval time between extremes C1 and C3 for the mentioned tests. The maximum value is 289 ms, while the minimum is 179 ms. The average value of the interval time between extremes C1 and C3 is approximately 205 ms.

Table 1S: Length of detected time intervals between extremes C1–C3.

# of eye mov.	# of areas in X axis	# of areas in Y axis	Interval length in X axis			Interval length in Y axis		
			C1-C3/a-b (ms)	C1-C3/a-b (ms)	C1-C3/a-b (ms)	C1-C3/a-b (ms)	C1-C3/a-b (ms)	C1-C3/a-b (ms)
1	2	1	**195**/281	**187**/304	-	**218**/234	-	-
2	2	-	**218**/320	**187**/289	-	-	-	-
3	1	2	**187**/242	-	-	**203**/289	**265**/328	-
4	1	1	**203**/250	-	-	**187**/265	-	-
5	2	2	**226**/289	**218**/296	-	**203**/281	**234**/312	-
6	1	2	**187**/273	-	-	**203**/281	**195**/296	-
7	3	1	**218**/390	**187**/242	**195**/210	**179**/242	-	-
8	2	1	**195**/296	**195**/304	-	**179**/273	-	-
9	3	1	**203**/343	**195**/351	**195**/281	**195**/265	-	-
10	2	3	**179**/210	**210**/226	-	**195**/257	**289**/382	**179**/250

Lekar a technika – Clinician and Technology 2020, vol. 50(3), pp. 101–113, DOI: 10.14311/CTJ.2020.3.04
ISSN 0301-5491 (Print), ISSN 2336-5552 (Online)

Table 2S shows the results of computed S3/S4 for all the diverse eye-blinking movements: (1) wink repeated three times, (2) wink repeated two times, (3) wink repeated two times, (4) single wink, (5) single wink, (6) wink repeated three times, (7) forced wink. As result, the lowest detected value is 2.9, so it was determined the referential value of 2.8.

Table 2S: Determination of empirical value for eyewink detection.

Eye-blinking number	**1**	**2**	**3**	**4**	**5**	**6**	**7**
S3/S4 (-)	3.1	3.4	4.1	**2.9**	4.1	3.5	3.3
S3/S4 (-)	3.9	3.7	4.2	-	-	4.1	-
S3/S4 (-)	3.8	-	-	-	-	3.9	-

Fig. 2S shows the "Detection of interval" GUI-window. In Fig. 2S, X1 is the result of EOG1-EOG2 signal subtraction, while Y1 is the result of EOG4-EOG3 signal subtraction; X2, and Y2 represent the low-pass filtering step; X3, and Y3 are the result of the second derivation to find out the acceleration values; and X4, and Y4 highlight the maximum and minimum signal values. Finally, X5 and Y5 are the results related to the detected time intervals.

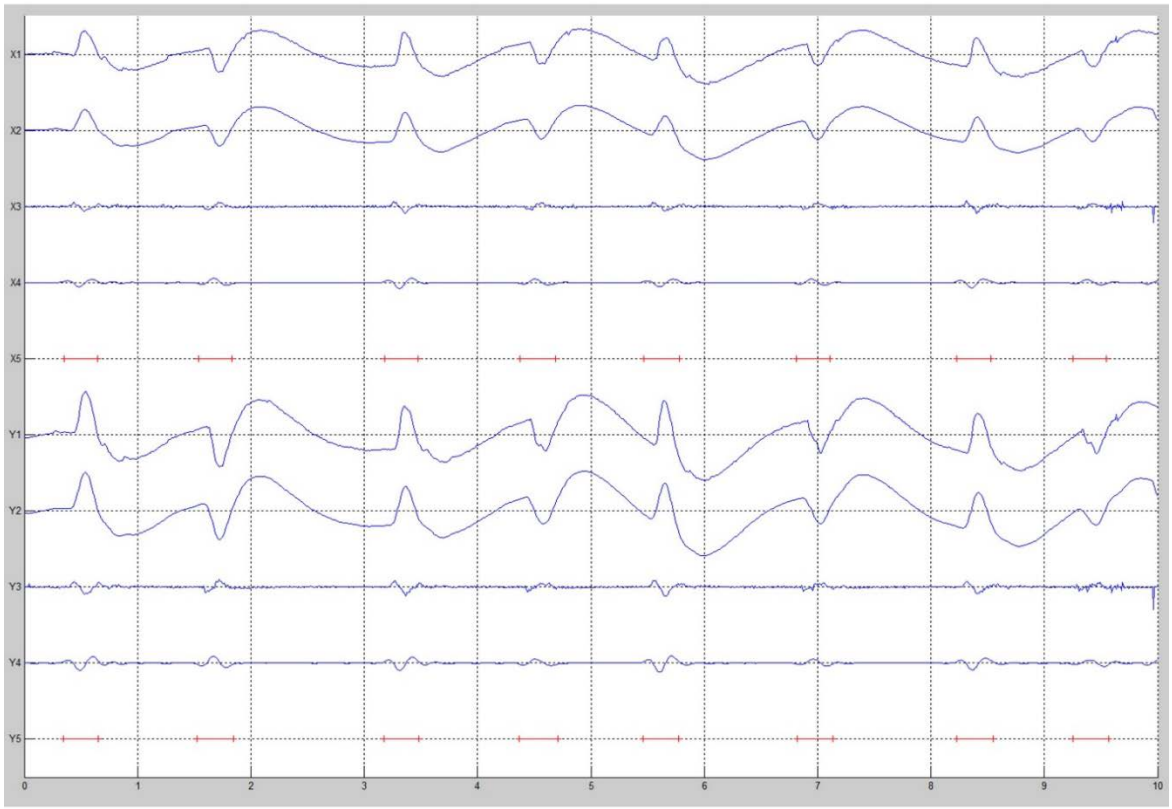

Fig. 2S: "Detection of interval" GUI-window.

Lekar a technika – Clinician and Technology 2020, vol. 50(3), pp. 101–113, DOI: 10.14311/CTJ.2020.3.04
ISSN 0301-5491 (Print), ISSN 2336-5552 (Online)

Fig. 3S shows the “DC component” GUI-window. In Fig. 3S, the blue lines are the signals before the filtration of the DC component, while the red lines show the signals after removing it.

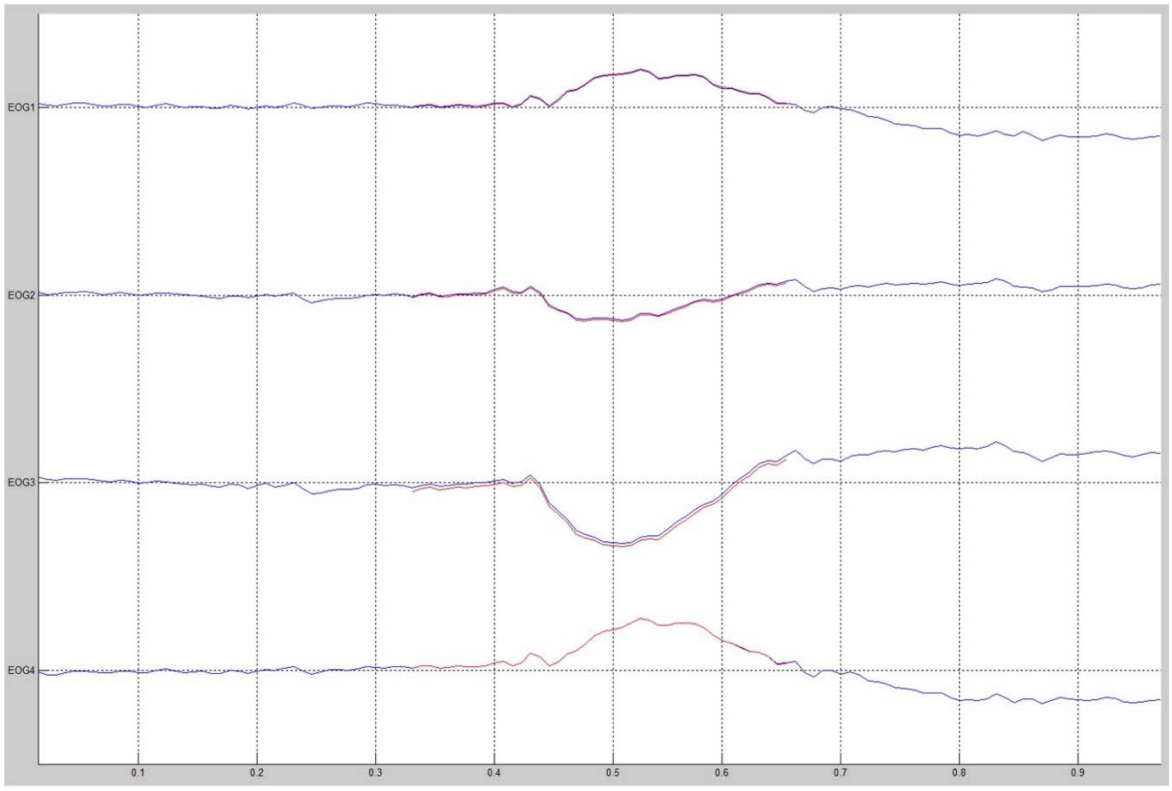

Fig. 3S: “DC component” GUI-window.

Fig. 4S shows the hardware of the EEG Wave Program, DEYMED Diagnostic s.r.o., formerly Alien technik s.r.o., which was used for measuring the EOG data and to record the video images during the experiment. Such a system was used to test and evaluate the MATLAB-based GUI developed in this work.

Fig. 4S: The experimental setup (left side); the hardware of the EEG Wave Program (right side).

Lekar a technika – Clinician and Technology 2020, vol. 50(3), pp. 101–113, DOI: 10.14311/CTJ.2020.3.04
ISSN 0301-5491 (Print), ISSN 2336-5552 (Online)

Fig. 5S shows the EOG signals acquired by using the EEG Wave Program for the eye movements number (18) single eye blink, three times.

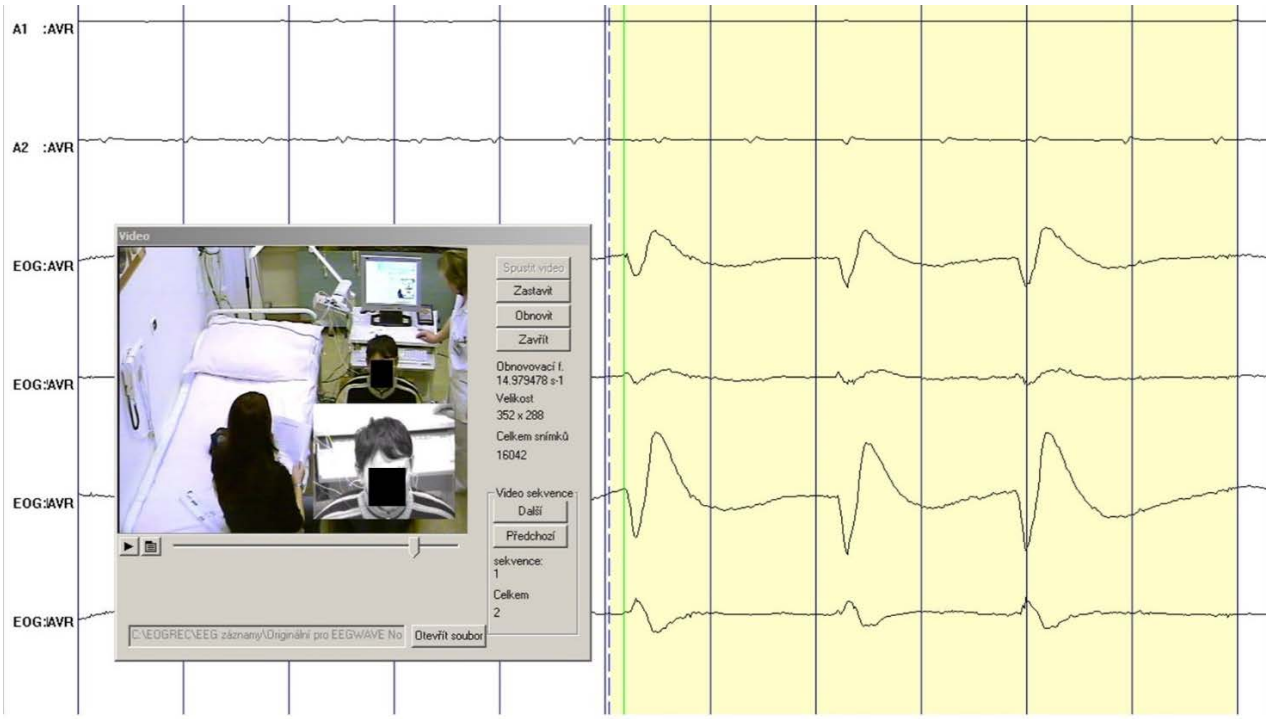

Fig. 5S: Validation of performed test for eye movement number (18) an eye blink, repeated three times.

References

[1] Du Bois-Reymond E. Untersuchungen über thierische Elektricität. Berlin: Reimer, 1848.

[2] Leigh RJ, Zee DS. The neurology of eye movements. 5th ed. Oxford University Press. 2015. ISBN: 9780199969289.

[3] Rayner K. Eye movements in reading and information processing: 20 years of research. Psychological Bulletin. 1998; 124(3):372–422. DOI: 10.1037/0033-2909.124.3.372

[4] Peter L, Janoscova B, Proto A, Cerny M. Electrooculography as a tool for managing application. In: IEEE International Conference on E-health Networking, Application & Services. Ostrava: IEEE Communications Society. 2018;1–5. DOI: 10.1109/HealthCom.2018.8531178

[5] Majaranta PA, Bulling A. Eye Tracking and Eye-Based Human–Computer Interaction. In: Fairclough, S.; Gilleade, K. Advances in Physiological Computing. Human–Computer Interaction Series. Springer, UK. 2014. DOI: 10.1007/978-1-4471-6392-3_3

[6] Singh H, Singh J. Human Eye Tracking and Related Issues: A Review. International Journal of Scienific and Research Publications. 2012;2(9):1–9. ISSN 2250-3153.

[7] Fejtova M, Fejt J, Lhotska L. Controlling a PC by eye movements: the MEMREC project. In: Proceedings of the Computers Helping People with Special Needs: 9th International Conference. Paris: Springer. 2004. DOI: 10.1007/978-3-540-27817-7_114

[8] Chen MC, Yu H, Huang ZL, Lu J. Rapid eye movement sleep behavior disorder. Current Opinion in Neurobiology. 2013;23(5):793–8. DOI: 10.1016/j.conb.2013.02.019

[9] Barnes D, McDonald WI. The ocular manifestations of multiple sclerosis. 2. Abnormalities of eye movements. Journal of Neurology, Neurosurgery, and Psychiatry. 1992;55(10):863–8. DOI: 10.1136/jnnp.55.10.863

[10] Nair G, Kim M, Nagaoka T, Olson DE, Thule PM, Pardue MT, Duong TQ. Effects of common anesthetics on eye movement and electroretinogram. Documenta Ophthalmologica. 2011; 122(3):163–76. DOI: 10.1007/s10633-011-9271-4

[11] Eggert T. Eye movement recordings: Methods. Developments in Ophthalmology. 2007;40:15–34, DOI: 10.1159/000100347

[12] Martinez-Cervero J, Ardali MK, Jaramillo-Gonzalez A, Wu S, Tonin A, Birbaumer N, Chaudhary U. Open Software/Hardware Platform for Human-Computer Interface Based on Electrooculography (EOG) Signal Classification. Sensors. 2020 May;20(9). DOI: 10.3390/s20092443

[13] Jaramillo-Gonzalez A, Wu S, Tonin A, Rana A, Ardali MK, Birbaumer N, Chaudhary U. A dataset of EEG and EOG from an auditory EOG-based communication system for patients in locked-in state. Scientific Data. 2021;8(1). DOI: 10.1038/s41597-020-00789-4

[14] Milanizadeh S, Safaie J. EOG-Based HCI System for Quadcopter Navigation. IEEE Transactions on Instrumentation and Measurement. 2020; 69(11):8992–9. DOI: 10.1109/TIM.2020.3001411

[15] Barbara N, Camilleri TA, Camilleri KP. A comparison of EOG baseline drift mitigation techniques. Biomedical Signal Processing and Control. 2020;57. DOI: 10.1016/j.bspc.2019.101738

[16] Thakor NV. Biopotentials and Electrophysiology Measurement. In: Webster, J.G. The Measurement, Instrumentation, and Sensors Handbook. vol. 74. CRC Press LLC, USA, 1999.

[17] Lopez A, Ferrero F, Valledor M, Campo JC, Postolache O. A study on electrode placement in EOG systems for medical applications. In: Proceedings of the IEEE International Symposium on Medical Measurements and Applications. Benevento. 2016. DOI: 10.1109/MeMeA.2016.7533703

[18] Aminoff M J. Aminoff's Electrodiagnosis in Clinical Neurology, 6th Ed.; Elsevier, 2012. ISBN: 9781455726769.

[19] Daly DD, Pedley TA. Current Practice of Clinical Electroencephalography, 2nd Ed.; Publisher: Raven Press, USA, 1990.

[20] Berg P, Scherg M. Dipole models of eye movements and blinks. Electroencephalography and Clinical Neurophysiology. 1991; 79(1):36–44. DOI: 10.1016/0013-4694(91)90154-V

[21] Ifeachor EC, Jervis BW, Allen EM, Morris EL, Wright DE, Hudson NR. Investigation and comparison of some models for removing ocular artefacts from EEG signals. Part 2 Quantitative and pictorial comparison of models. Medical and Biological Engineering and Computing. 1988;26(6):591–8. DOI: 10.1007/BF02447496

[22] Gasser T, Sroka L, Mocks J. The Correction of EOG Artifacts by Frequency Dependent and Frequency Independent Methods. Psychophysiology. 1986;23(6):704–12. DOI: 10.1111/j.1469-8986.1986.tb00697.x

[23] Kohonen T. Self-organising maps. Berlin: Springer, 1995. ISBN 3-540-58600-8.

[24] Ileri R, Latifoglu F, Demirci E. New Method to Diagnosis of Dyslexia Using 1D-CNN. In: Proceedings of the Medical Technologies Congress, TIPTEKNO. Antalya. 2020. DOI: 10.1109/TIPTEKNO50054.2020.9299241

[25] Liebich S, Bruser C, Leonhardt S. Deconvolution-based physiological signal simplfication for periodical parameter estimation. Lékař a technika-Clinician and Technology. 2014; 44(2):18–24.

[26] Conforto S, D'Alessio T. Spectral analysis for non-stationary signals from mechanical measurements: a parametric approach. Mechanical Systems and Signal Processing. 1999;13(3):395–411. DOI: 10.1006/mssp.1998.1220

[27] Penhaker M, Stula T, Cerny M. Automatic Ranking of Eye Movement in Electrooculographic Records. In: Proceedings of the 2nd IEEE International Conference on Computer Engineering and Applications. Bali Island, 2010. DOI: 10.1109/ICCEA.2010.238

[28] EEG Wave Program. Accessed: Feb. 08, 2021. [Online]. Available: https://deymed.cz/truscan-eeg

Antonino Proto, Ph.D.
Dept. of Cybernetics and Biomedical Engineering
Faculty of Electrical Engineering & Computer Science
VSB-TU Ostrava
17. listopadu 2172/15, CZ-708 00 Ostrava

E-mail: antonino.proto@vsb.cz
Phone: +420 597 325 991

Lekar a technika – Clinician and Technology 2020, vol. 50(3), pp. 101–113, DOI: 10.14311/CTJ.2020.3.04
ISSN 0301-5491 (Print), ISSN 2336-5552 (Online)